ECMWF Feature article

from Newsletter Number 136 – Summer 2013

METEOROLOGY

Breakthrough in forecasting equilibrium and non-equilibrium convection

www.ecmwf.int/en/about/news-centre/media-resources

doi:10.21957/8j0xcrpk

This article appeared in the Meteorology section of ECMWF Newsletter No. 136 – Summer 2013, pp. 15–22.

Breakthrough in forecasting equilibrium and non-equilibrium convection

Peter Bechtold, Noureddine Semane, Philippe Lopez, Jean-Pierre Chaboureau, Anton Beljaars, Niels Bormann

A new diagnostic convective closure has been developed. Important improvements in global NWP forecasts have been obtained with the new convective closure. In particular, there is not only a better representation of the diurnal cycle of convection, but also a better depiction of its spatial distribution.

A comparison of low-resolution seasonal integrations and high-resolution short-range forecasts against satellite and radar data shows that with the new convective closure it is possible to realistically represent non-equilibrium convection. Other investigations, which involve comparisons with a cloud resolving model (CRM) for the Sahel region and with satellite data, confirm the good performance of the new scheme.

The new convective closure is dependent on an extended convective available potential energy (CAPE). It has been derived under a quasi-equilibrium assumption for the free troposphere subject to boundary-layer forcing. The simple closure involves adjustment time-scales for the free troposphere and the land and ocean boundary-layers.

Equilibrium and non-equilibrium convection

Equilibrium convection is generally interpreted as indicating that the convection is in equilibrium with the forcing due to the mean advection and processes other than convection. In other words, the convection can react on time scales short enough for the residual tendency between the forcing and the convective stabilization to be small. This is generally referred to as quasi-equilibrium. Numerous theoretical and experimental studies have confirmed the validity of quasi-equilibrium for synoptic disturbances and for time-scales of the order of one day. Today most global numerical weather prediction (NWP) and climate models employ a convection parametrization based on the quasi-equilibrium assumption – see Box A.

In contrast to equilibrium convection, the forcing of non-equilibrium convection varies typically on time scales of a few hours. Non-equilibrium convection under rapidly-varying forcing typically occurs when either the upper-tropospheric forcing is strong and the convection is inhibited by a capping inversion, or the upper-level forcing is weak and the precipitating convection is driven along its trajectory by rapidly-varying and strong surface heat fluxes. The large-scale flow, in turn, readjusts to the convective heat source by a process called geostrophic adjustment that operates via inertia-gravity waves on time-scales of a few hours. Forecasting non-equilibrium convection is challenging for models, and this is particularly true for surface forced convection where the mid- to upper-tropospheric vertical motions are the response to and not the driver of deep convection.

Convection parametrization

A

Most convection parametrization schemes are based on the concept that vertical mass transport occurs in convective plumes which exchange mass with their environment. In these schemes the rate of horizontal mass exchange has to be specified, and the mass flux at cloud base is determined from the assumption of convective quasi-equilibrium. In spite of employing a similar basic convective framework, the models can produce substantially different large-scale tropical wave spectra and intra-seasonal variability such as the Madden-Julian oscillation. However, *Bechtold et al*. (2008) and *Jung et al.* (2010) demonstrated with ECMWF's Integrated Forecasting System (IFS) that the basic mass flux framework under the quasi-equilibrium assumption provides a realistic reproduction of the observed middle-latitude synoptic variability, as well as the tropical wave spectra and intra-seasonal variability.

doi:10.21957/8j0xcrpk

Diurnal cycle of convection

The diurnal cycle of convection is probably the most prominent manifestation of non-equilibrium convection driven by the boundary-layer. Numerous observational studies and those based on cloud resolving models (CRMs) have been devoted to the diurnal cycle of convection over land. The phase of the diurnal cycle can vary strongly on regional scales, though the general picture is that of a morning shallow convective phase, followed by a gradual onset of deeper convection, with rain rates peaking in the late afternoon to early evening. It has been found that the phase and intensity of precipitation mainly depends on the surface fluxes and lower to mid-tropospheric stability and moisture, but boundary-layer processes such as convergence, gravity waves and cold pools also play a role in the onset and propagation of deep convection. In addition, it has been shown that CRMs with resolutions of order 2.5 km or higher, as also used by many of our Member States for their regional short-range forecasts, are able to reproduce the observed diurnal cycle (*Langhans et al.,* 2012) though the high-resolution forecasts are sensitive to the formulation of the horizontal turbulent mixing.

The same success in reproducing the observed diurnal cycle can generally not be reported for large-scale models. Indeed, numerous global and regional model studies point to systematic errors in the diurnal cycle of precipitation when a convection parametrization scheme is employed, namely a too early onset of deep convection with a diurnal cycle of precipitation that is roughly in phase with the surface fluxes. These problems have also persisted in the IFS over the last decades. The diurnal cycle of non-precipitating shallow convection, however, can be realistically represented with a quasi-equilibrium closure for the boundary-layer and a prognostic cloud scheme, as demonstrated with the IFS by *Ahlgrimm & Forbes* (2012).

Various approaches have been taken to improve the representation of convection driven by surface fluxes focusing on the entrainment rates, the convective triggering and particularly the convective closure. New closure formulations include the convective inhibition (CIN), lifting by cold pools, environmental moisture, and also prognostic formulations with convective memory. However, so far none of the above methods have proved to be general and robust enough to replace, at least in the global NWP context, the standard equilibrium closures for the CAPE.

It is pleasing that it has been possible to develop a convective closure that extends the current CAPE closure in the IFS and, as outlined below, realistically represents both synoptically and boundary-layer forced convection.

CAPE and convective closure

The CAPE (J kg^{-1}) is defined as the vertical integral, from the cloud base to the cloud top, of the acceleration a moist air parcel experiences due to the density deficit with respect to its dry environment. The World Meteorological Organization's definition of CAPE assumes that the cloudy parcel does not mix with the environment. With this definition typical values of CAPE, as available from the ECMWF archive, are on the order of 1000 J kg^{-1}. However, in the context of convection parametrization, we use the more representative CAPE of an entraining parcel which has typical values of order 100 J kg^{-1}.

CAPE is produced in the free troposphere by:

- Cooling through mean large-scale advection and cooling from radiation, both affecting the large-scale environment.
- Surface heat and moisture fluxes, affecting the height of the cloud base and the properties of the rising parcel (updraught).

In the case of weak large-scale forcing the CAPE varies essentially with the surface fluxes. Therefore, a convection scheme that determines the convective intensity from the assumption that convection consumes all CAPE over a convective time-scale (typically of order 1 hour) tends to produce a diurnal cycle of precipitation that follows the surface fluxes. Over land this obviously does not correspond to the observations. The IFS also uses such a closure which in the following is referred to as CTL.

The NEW closure that has been developed uses an effective CAPE that recognizes that not all the boundary-layer heating is available to be converted into deep precipitating motions, but only a fraction, while the main part during the morning and noon is balanced by dry and shallow non-precipitating convection. The effective CAPE, which accounts for the imbalance between shallow near-surface heating and deep convective motions, can be computed by assuming different adjustment time-scales for the free troposphere and the boundary-layer. Over land the boundary-layer time-scale is set to the convective turnover time scale (defined as the ratio between cloud depth and mean updraught speed), while over water it is set to the advective time-scale (ratio of cloud base height to mean wind speed in the boundary-layer).

Convective closure aims to determine through scaling the actual mean mass flux and precipitation of a population of convective up- and downdraughts. While simple parcel theory (CAPE) is obviously not sufficient to determine the ensemble mean properties of convection in non-equilibrium surface forced convection, the NEW closure effectively corrects for these deficiencies.

Climatology of the diurnal cycle of precipitation

The diurnal cycle of convection in the IFS is first evaluated from an ensemble of one-year integrations and compared against a ten-year precipitation climatology from the Tropical Rainfall Measurement Mission (TRMM) for June, July and August. The simulations are forced by analysed sea surface temperatures, and use spectral truncation T159 (gridlength 125 km) with 91 vertical levels, and a time step of 1 hour. Precipitation data from both the simulations and the observations are composited in hourly bins, and the diurnal amplitude and phase are computed from the first harmonic of a Fourier series.

The diurnal amplitude (mm day^{-1}) of the precipitation in the tropical belt from the TRMM radiometer is displayed in Figure1a. Maximum amplitudes reach around 10 mm day^{-1} over tropical land.

Amplitudes from the model integrations using the CTL and NEW closures are displayed in Figures 1b and 1c. Overall, the spatial distribution of the amplitudes is reasonably reproduced in both simulations, but the amplitudes reach higher values than the TRMM-based observations, particularly over northern Amazonia. However, the simulated total rainfall over Amazonia appears realistic when compared to the Global Precipitation Climatology Project 2.2 dataset (not shown).

The corresponding phase of the diurnal cycle (LST) is displayed in Figure 2. As already discussed in earlier studies, maximum precipitation in the TRMM radar data (Figure 2a) occurs over tropical land roughly in the late afternoon to early evening, though strong regional variations are present. In particular, convective rainfall over Amazonia may peak as early as local noon due to the high relative humidity and low stability in the lower troposphere. In contrast, maximum precipitation over the tropical oceans occurs during the early morning. The CTL closure (Figure 2b) provides a reasonable reproduction of the diurnal phase over water, but the convective precipitation over land generally peaks around local noon.

However, as shown in Figure 2c, a marked improvement is obtained with the NEW closure that shifts the diurnal cycle over land by 4–5 hours compared to CTL, and also improves the diurnal cycle in coastal regions (e.g. off the Central American and West African coasts, as well as off the Indian subcontinent and over the Maritime Continent). Experimentation shows that the improvements over coastal regions are primarily due to a better representation of the convection generated over land and advected over sea, along with the associated subsiding motions, but the modified adjustment over sea also contributes.

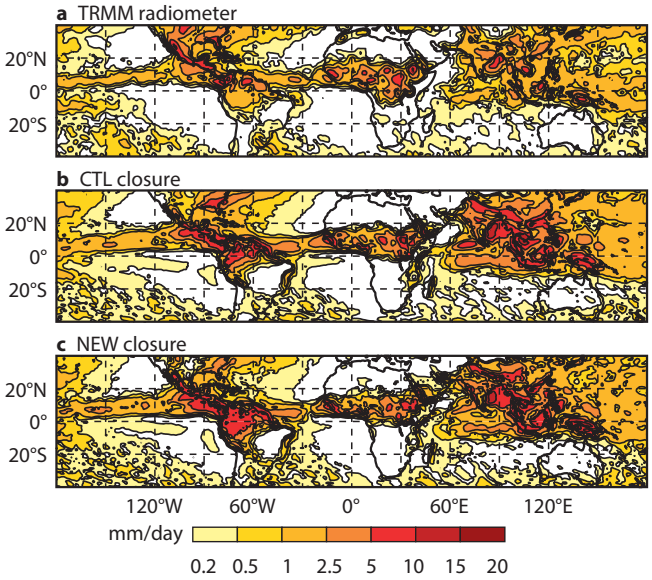

Figure 1 Diurnal amplitude (mm day^{-1}) of the precipitation in the tropical band as obtained (a) from a 10-year climatology of TRMM radiometer data for June, July and August (courtesy Yukari Takayabu and colleagues), and from an ensemble of annual IFS integrations with (b) the CTL and (c) NEW closures at T159 (gridlength 125 km).

doi:10.21957/8j0xcrpk

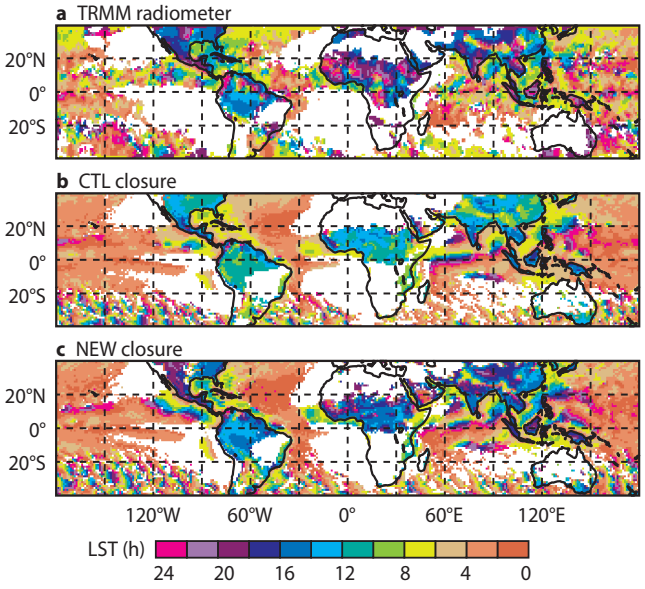

Figure 2 Same as Figure 1, but for the diurnal phase (LST) of the precipitation. Also, TRMM radar data has been used instead of the radiometer data.

High-resolution forecasts of the diurnal cycle of precipitation

In addition to seasonal integrations, higher resolution daily 3-day forecasts have been performed for June, July and August 2011 and 2012 at T511 (gridlength 40 km) with 137 vertical levels and a time step of 900 s. The forecasts were initialised from ECMWF's operational analyses at T1279 (gridlength 16 km) with 91 levels. The forecasts are compared to the NCEP Stage IV composites obtained from the combination of radar and rain gauge data (NEXRAD, hereafter) over the continental United States during summer 2011 and 2012, and German radar composites from the Deutsche Wetterdienst for summer 2011. All forecast days have been used to compute the diurnal composites that are three times 90 days for each summer season.

The amplitude and phase of the diurnal cycle of precipitation averaged over the summers 2011 and 2012 are depicted in Figure 3 and Figure 4 for the continental United States. Numerous previous studies have already described the diurnal cycle over this region. In summary, as is also evident from the NEXRAD data (Figure 3a and Figure 4a), the diurnal cycle over the continental United States is characterized by three distinctive regions.

- Rocky Mountain area, where convective activity peaks during the late afternoon.
- Central Planes with predominantly night-time convection from propagating mesoscale convective systems triggered over the Rocky Mountains.
- Eastern United States and coastal regions with predominantly late afternoon convection and a particularly strong diurnal amplitude over the Florida peninsula.

The CTL forecasts have quite a reasonable representation of the spatial variations in the amplitude (Figure 3b), but underestimate the amplitude east of the mountain ridge and somewhat overestimate the amplitude in the coastal regions. The results with the NEW forecasts (Figure 3c) are rather similar though slightly improve on the CTL. However, concerning the phase, the NEW forecasts (Figure 4c) substantially delay the diurnal cycle by 4–5 hours compared to CTL (Figure 4b) so that the results more closely match the observations. But over the Eastern United States the diurnal cycle in NEW still precedes the observed cycle by up to 2 hours.

To give an overview of the diurnal cycle in the high-resolution short-range forecasts, the area-averaged diurnal rainfall composites are depicted in Figure 5 for the Eastern United States and Germany and also for the central Sahel region, which has TRMM climatological data for comparison. The area-averaged representation for all three locations shows that NEW has quite a good fit to the daytime and evening diurnal cycle of precipitation, shifting it by up to 6 hours compared to CTL. The late night precipitation, however, remains underestimated in both NEW and CTL in spite of having the convection parametrization coupled to a prognostic cloud scheme. This precipitation deficit might be due to the missing representation of convective system dynamics including spreading surface cold pools and predominantly upper-level mesoscale lifting during the night.

Over the Sahel (Figure 5c), NEW realistically increases the precipitation with respect to CTL. A correct phase representation of the diurnal cycle is particularly important in this region where the convective heating is a key driver of the meridional pressure gradient and the large-scale dynamics.

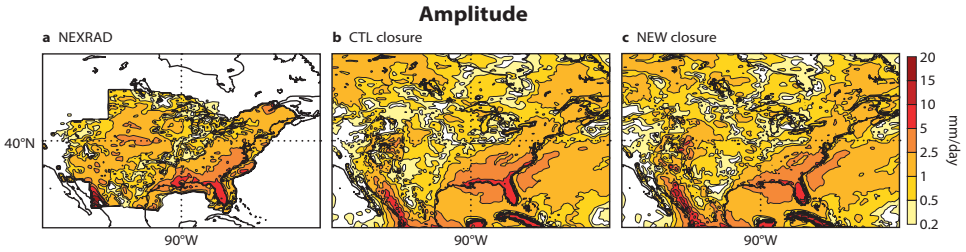

Figure 3 Amplitude (mm day^{-1}) of the precipitation averaged over June, July and August 2011 and 2012 for the continental United States from (a) NEXRAD, and from daily 72-hour forecasts with (b) CTL and (c) NEW closures at truncation T511 (gridlength 40 km).

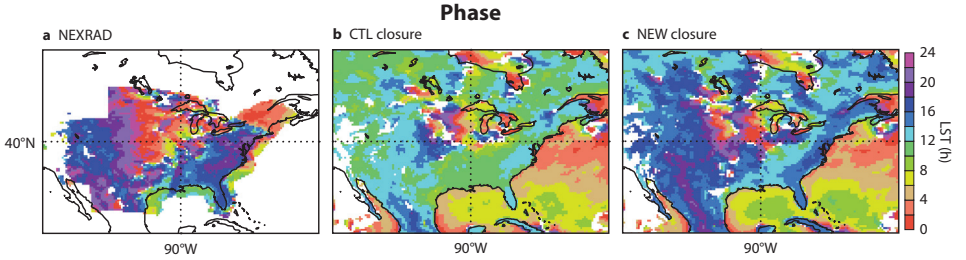

Figure 4 Same as for Figure 3, but for the diurnal phase of the precipitation (LST).

Heating and moistening profiles

The convective heating and its dynamical response are investigated over the central Sahel region using CRM data from the Meso-NH limited area model (*Lafore et al.,* 1998) that has been run during 10–25 June 2012 at 2.5 km grid-spacing daily for 24-hours over a domain that is roughly 2,200 km by 1,700 km. The CRM uses the same ECMWF T1279 analyses as initial conditions as are used for CTL and NEW. In addition, the CRM open boundaries are updated every 6 hours from the ECMWF analyses.

The heating and moistening rates (K day^{-1}) shown as shaded in Figure 6 are the total heating less the radiation (traditionally called the apparent heat source Q1-Qrad) and the total moistening (traditionally called the apparent moisture source –Q2).

One recognizes for both CTL and NEW (Figures 6a & 6c) a distinctive phase with deep boundary-layer heating from 6:30 to 12 LST, followed by boundary-layer cooling and more elevated dry and shallow convective heating lasting until 17 LST. Boundary-layer moistening (Figures 6b & 6d) lasts until about 9 LST. It is followed by strong drying of the lower boundary-layer, and dry and shallow convective moistening of the lower troposphere extending to or exceeding the 600 hPa level at 15–16 LST.

During the strong growth phase of the boundary-layer from 10–17 LST, corresponding to a continuous growth of CAPE, the heating in the upper part of the boundary-layer is in balance with the cooling due to adiabatic motions, but the upper-troposphere is not in equilibrium. Indeed, the evolution of the upper-tropospheric heating profiles differs strongly between CTL and NEW. Whereas in CTL the mid-to upper-tropospheric heating of 5–10 K day^{-1} from precipitating deep convection occurs around 13 LST, and therefore during the growth of the boundary-layer, the strong deep convective heating in NEW occurs when the lower- to middle-troposphere has reached its maximum total heat content.

The dynamic response to deep convective heating is a couplet of upper-tropospheric cooling and lower-tropospheric warming, which through the quasi-geostrophic adjustment process becomes effective a few hours after the convective heating. This dynamic cooling/heating couplet is particularly important for the formation of mesocale stratiform rain during night. The upper-tropospheric response in NEW is clearly delayed, and is stronger than in CTL, attaining values of -4 K day^{-1}. Nevertheless, NEW still underestimates the night-time precipitation with respect to the observations (Figure 5).

A comparison of the heating and moistening profiles with CRM data (Figures 6e & 6f) reveals that NEW produces a realistic diurnal cycle in phase and amplitude, including the shallow and congestus heating phase, though the latter is less pronounced in the CRM. The heating profiles (Figures 6c & 6e) are also in fair agreement with the observed cloud evolution during days with late afternoon convection *(Zhang & Klein, 2010)*. The moistening rates (Figures 6d & 6f) are also in good agreement during daytime. However, larger differences in the heating profiles between the CRM and the IFS exist in the early morning hours which can be partly attributed to boundary-layer spin-up processes in the CRM.

Overall, we think that the structure and evolution of the convective heating and its dynamical response using NEW compares fairly well with the results from the CRM, given the limited domain size of the CRM and its sensitivity to the parametrization of horizontal mixing.

doi:10.21957/8j0xcrpk

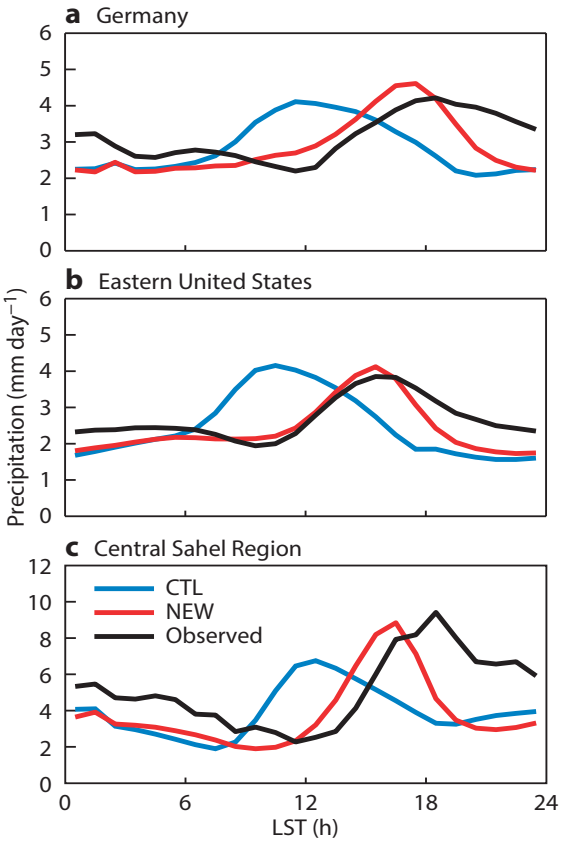

Figure 5 Diurnal composites of area-averaged total precipitation (mm day^{-1}) from CTL and NEW against observations for (a) Germany [48°–52°N, 7°–14°E] using DWD radar, (b) eastern United States [30°–45°N, 100°–80°W] using NEXRAD, and (c) central Sahel region [5°–20°N, 10°–30°E] using TRMM climatological radiometer data. The observations are for June, July and August 2011 for (a) and June, July and August 2011 and 2012 for (b) and (c).

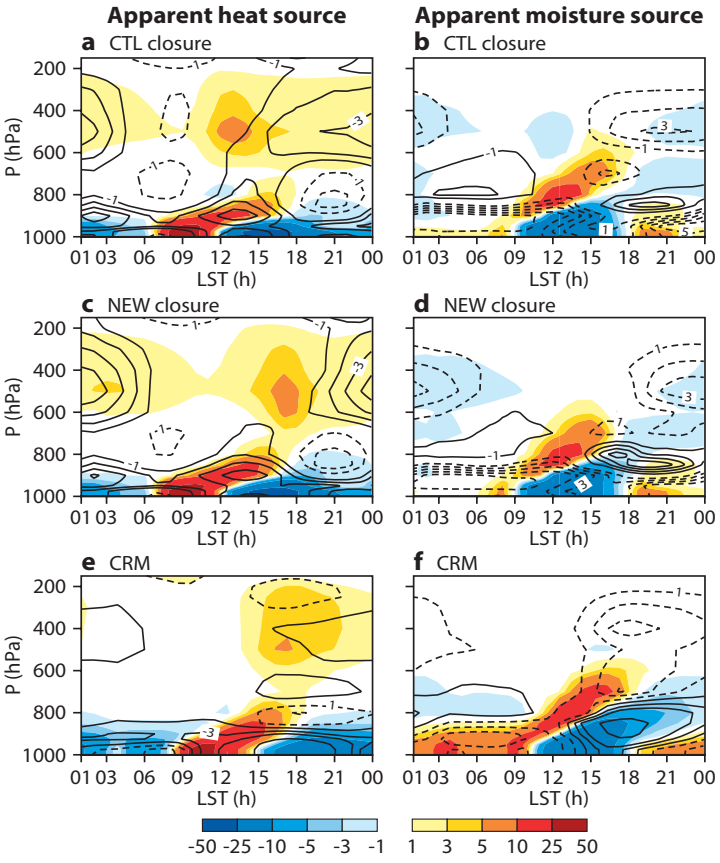

Figure 6 Diurnal composites of heating rate (left panels) and moistening rate (right panels)) over the central Sahel for CTL (top panels), NEW (middle panels), and from the CRM (bottom panels) during 10–25 June 2012. Total heating rate minus radiation (Q1-Qrad) and total moistening rate (-Q2) are shaded. Solid contour lines denote cooling and drying rates due to adiabatic motions and dashed contour lines (interval 1 K day^{-1}) denote adiabatic heating and moistening.

doi:10.21957/8j0xcrpk

Comparison with satellite data

A global picture of the improvement in the heating structure of NEW compared to CTL is presented in Figure 7 using July 2012 as an illustration. This shows a reduction in root-mean-square (rms) error of the brightness temperatures (BTs) when evaluating the short-range (first-guess) forecasts during the 12-hour assimilation window against the clear-sky BTs from AMSU-A microwave sounders on board sun-synchronous NOAA satellites. The satellites have different twice-daily overpass times, and the results are shown for two channels, sensitive to temperature over broad atmospheric layers around 500–1000 hPa and 250–600 hPa. Clearly, NEW provides an improvement over CTL over most land regions with persistent active convection, and in particular in the middle to upper-troposphere where the convective heating is strongest. The improvement of order 0.1 K is primarily a result of a reduction in the bias for the day-time overpasses. It is small in absolute values, but it is statistically significant, and has to be compared to the absolute rms error of the 12-hour forecasts that does not exceed 0.3 K. The areas of reduction in the short-range forecast errors are consistent with the improvements in the diurnal cycle seen in the long integrations (Figure 2).

The improvements in the diurnal cycle in NEW can also be easily identified on infrared satellite imagery. As an illustrative example, Figure 8 shows the observed 10.8 μm infrared satellite images over Europe at 12 and 18 UTC on 1 July 2012 from Meteosat 9 and the synthetic forecast images from the CTL and NEW short-range forecasts at T1279 (gridlength 16 km).

The satellite images show synoptically-forced convection over western and central Europe, and surface-forced convection over the Balkans and the Atlas Mountains, a situation that is frequently observed during summer. Indeed, CTL overestimates the convection over Eastern Europe and the Balkans at 12 UTC and underestimates the convection in these areas and the Atlas Mountains at 18 UTC. In contrast, NEW clearly better reproduces the daytime convective evolution and also better represents the localisation and structure of convection. Due to the higher CAPE values in NEW, the convection is more coarse-grained with higher local convective rain intensities during late afternoon. A separate comparison of NEW with CRM data revealed that the higher daytime convective rain intensities in NEW are more realistic than the more large-spread, but weaker rain events in CTL.

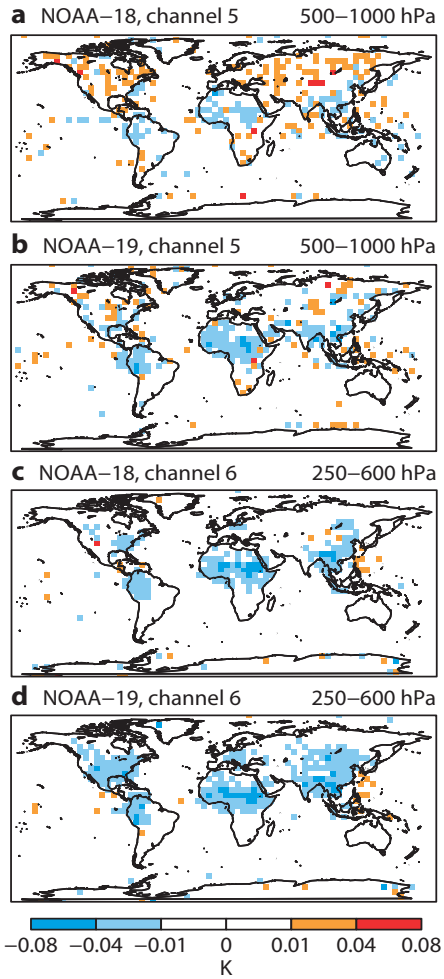

Figure 7 Root mean square error differences in clear-sky brightness temperatures for July 2012 between NEW and CTL during the 12-hour window of the 4D-Var analysis, when evaluated against AMSU-A microwave sounding channels onboard NOAA sun-synchronous satellites. The channels are representative for different atmospheric layers: (a) and (b) NOAA-18 and 19 channel 5 for the 500–1000 hPa layer, and (c) and (d) NOAA-18 and 19 channel 6 for the 250–600 hPa layer. The twice daily overpass times are 03 LST and 15 LST for NOAA-18, and 01:30 LST and 13:30 LST for NOAA-19.

doi:10.21957/8j0xcrpk

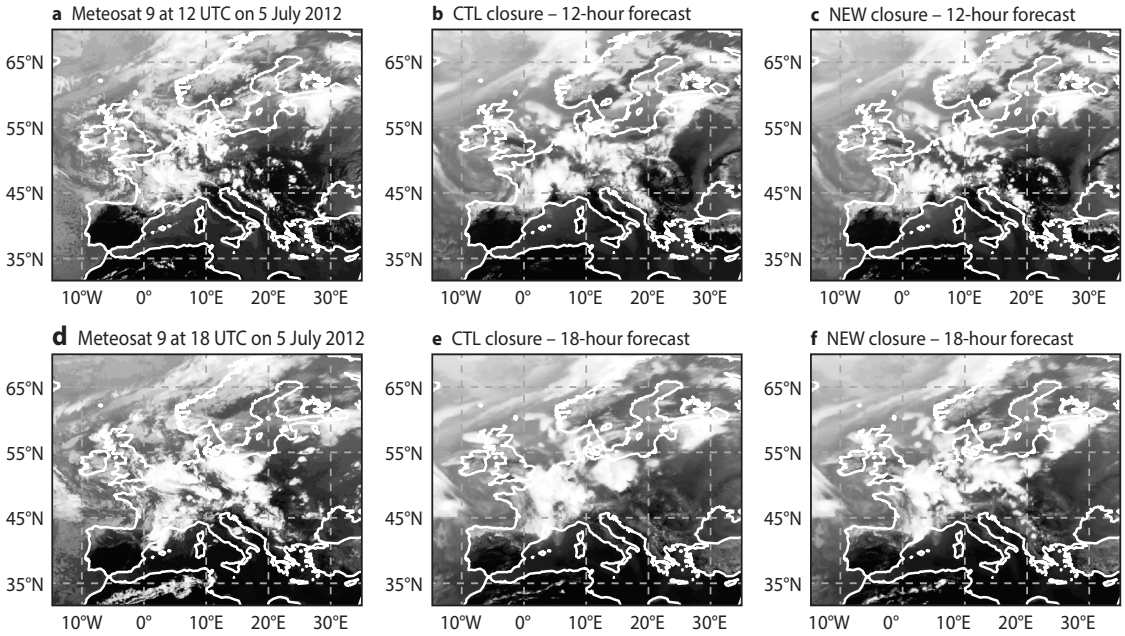

Figure 8 (a) Infrared 10.8 μm satellite image from Meteosat 9, channel 9 over Europe on at 12 UTC on 5 July 2012 along with the 12-hour forecasts from (b) CTL and (c) NEW closures at truncation T1279 (gridlength 16 km). (d) As (a) but for 18 UTC on 5 July 2012. (e), (f) As (b), (c) but for 18-hour forecasts. All images are at resolution 0.2°.

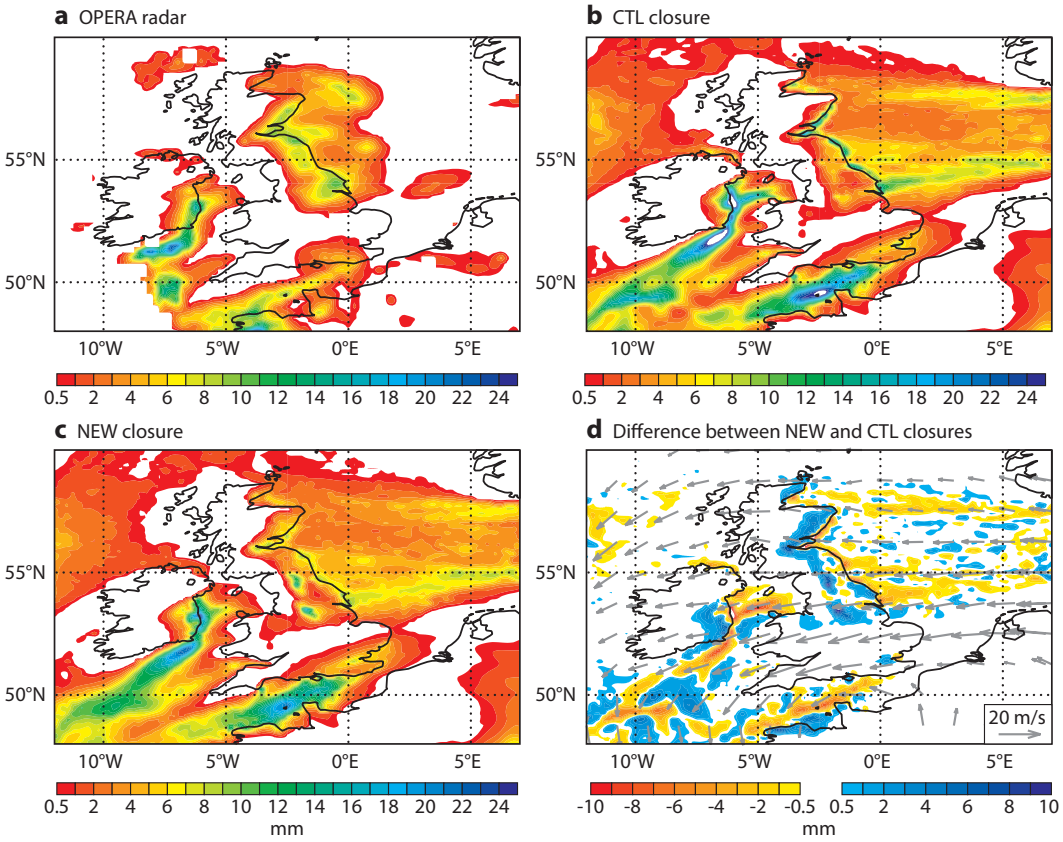

Figure 9 24-hour precipitation accumulations (mm) for 1 December 2010 over the British Isles and near European mainland from (a) radar observations on a 0.25° grid, and 24-hour forecasts with (b) CTL and (c) NEW at truncation T1279 (gridlength 16 km). (d) The difference between NEW and CTL closures. The advection is represented in (d) by the mean 500–850 hPa wind.

doi:10.21957/8j0xcrpk

Convection over the oceans and wintry showers

So far, there has been little discussion on the effect of NEW over the oceans. In these areas, the overall synoptic impact can be described as largely neutral, including the medium-range forecasts of tropical cyclones and the representation of the Madden-Julian oscillation in seasonal integrations. However, there is a positive impact on the representation of convection and the diurnal cycle in near-coastal areas. Of particular concern in NWP is, for example, the inland advection of wintry showers forming over the relatively warm sea. This is illustrated by considering the 24-hour precipitation accumulations over the British Isles and the near European mainland on 1 December 2010 as observed from ground-based radar (Figure 9a) along with the 24-hour forecasts for CTL (Figure 9b) and NEW (Figure 9c) at T1279.

Nearly all precipitation accumulated as snow on the ground, reached up to 20 cm and was predominantly of the convective type. Clearly, NEW reduces the unrealistically strong snowfall along the coast by up to 50% compared to CTL and more realistically moves the convective snowfall inland, bringing up an extra of 10 cm snow (Figure 9d). This is possible even with a diagnostic formulation of convection as the moist unstable air is advected inland, and the simulated convection is formulated so that it is allowed to depart from elevated layers. The main difference between NEW and CTL is the slower convective adjustment, avoiding a too strong large-scale response leading to coastal convergence.

Benefits and challenges

Important improvements in global NWP have been obtained with a new convective closure, which is dependent on the convective available potential energy CAPE and assumes a quasi-equilibrium for the free troposphere subject to boundary-layer forcing. With this formulation only at the end of the lower tropospheric heating and moistening cycle is the entire CAPE available for conversion into deep convective motions. Consequences for NWP are not only a better phase representation of convection, but also better forecasts of its spatial distribution and local intensity.However, the representation of the night-time precipitation that is related to a mesoscale lifting/subsidence couplet in the upper-troposphere remains a challenge in convection forecasting. With parametrized convection the night-time precipitation is underestimated. Future improvements in this bias might be achieved by a tighter coupling between the microphysics in the convection and the resolved microphysics, or a more prognostic formulation of convection.

Finally, concerning future higher-resolution upgrades of the IFS, from the current T1279 (16 km) operational resolution to the envisaged T3999 (5 km) resolution in 2020, we think that the new convective closure will enable a smooth transition from parametrized to resolved deep convection in both the forecasts and the data assimilation as there is no longer a substantial discrepancy in the phase and location between parametrized and resolved convection.

Further reading

Ahlgrimm, **M.** & **R. Forbes,** 2012: The impact of low clouds on shortwave radiation in the ECMWF model. *Mon. Weather Rev.,* **140**, 3783–3794.

Bechtold, P., M. Köhler, T. Jung, F. Doblas-Reyes, M. Leutbecher, M. Rodwell, F. Vitart & **G. Balsamo,** 2008: Advances in simulating atmospheric variability with the ECMWF model: From synoptic to decadal time-scales. *Q. J. R. Meteorol. Soc.*, **134**, 1337–1351.

Jung, T., G. Balsamo, P. Bechtold, A. Beljaars, M. Köhler, M. Miller, J.-J. Morcrette, A. Orr, M. Rodwell & **A. Tompkins,** 2010: The ECMWF model climate: recent progress through improved physical parametrizations. *Q. J. R. Meteorol. Soc.*, **136**, 1145–1160.

Lafore, J.-P., J. Stein, N. Asencio, Ph. Bougeault, V. Ducrocq, J. Duron, C. Fischer, P. Héreil, P. Mascart, V. Masson, J.-P. Pinty, J.-L. Redelsperger, E. Richard & **J. Vilà-Guerau de Arellano,** 1998: The Meso-NH Atmospheric Simulation System. Part I: adiabatic formulation and control simulations. Scientific objectives and experimental design. *Annales Geophysicae*, **16**, 90–109.

 doi:10.21957/8j0xcrpk